VNUHCM Journal of Engineering and Technology 2026, 9(3):3067-3078

Open Access Full Text Article

Research Article

Research and design two-axis profile scanning control system supporting fiber laser welding technology

Trong-Khuyen Nguyen[1], Duy-Anh Nguyen[2,3], Quang-Phuoc Tran[2,3,*]

[1]Control, Automation in Production and Improvement of Ttechnology Institute, 89B Ly Nam De Street, Hoan Kiem District, Hanoi City, Vietnam

[2]Faculty of Mechanical Engineering, Ho Chi Minh City University of Technology (HCMUT), Vietnam

[3]Vietnam National University Ho Chi Minh City, Ho Chi Minh City, Vietnam

Correspondence

Quang-Phuoc Tran, Faculty of Mechanical Engineering, Ho Chi Minh City University of Technology (HCMUT), Vietnam

Vietnam National University Ho Chi Minh City, Ho Chi Minh City, Vietnam

Email: tqphuoc@hcmut.edu.vn

History
- Received: 06-08-2023
- Revised: 10-11-2023
- Accepted: 07-08-2025
- Published Online: 03-08-2026

DOI : https://doi.org/10.32508/vnuhcmj-et.v9i3.1141

Check for updates

ABSTRACT

This research paper presents a comprehensive investigation into the design and development of a cutting-edge two-axis profile scanning control system tailored explicitly for fiber laser welding technology. The system incorporates two reflecting galvanometer mirrors, which play a pivotal role in achieving precise and intricate laser profiles, effectively addressing the inherent challenges of controlling heat application in welding processes. With the mathematical model of the control system carefully formulated, encompassing forward and inverse kinematic equations that govern the rotational angles of the mirrors, these equations establish the fundamental relationship between the movements of the mirrors and the resulting laser profiles, facilitating a deeper understanding of the control mechanisms. To ensure optimal performance, an advanced control algorithm is proposed to efficiently manage the mirrors' motions, carefully considering sampling time and operational limitations, thus providing a comprehensive and effective approach to control the system. Extensive MATLAB simulations are conducted to evaluate the effectiveness and accuracy of the algorithm, providing tangible evidence of its ability to achieve precise and customizable laser profiles. The two-axis profile scanning control system demonstrates significant advantages over conventional welding methods, offering unparalleled flexibility and control over welding geometries. This versatility enables the welding of delicate materials and complex components with exceptional accuracy and minimal heat loss, thereby expanding the range of applications in various industries, including automotive, electronics, and medical devices. Beyond the realm of welding, the developed control system exhibits immense potential for broader applications in material processing, additive manufacturing, and high-precision fabrication processes, further solidifying its position as a transformative tool in modern manufacturing and automation. In conclusion, this research paper represents a critical contribution to the advancement of fiber laser welding technology by introducing a cutting-edge two-axis profile scanning control system. The system's ability to generate precise and intricate laser profiles has the potential to revolutionize metal joining processes, empowering manufacturers with greater flexibility and control over weld geometries, and its broader applicability in high-precision applications holds promise for a wide range of industries, marking a significant step towards the realization of advanced and efficient manufacturing practices.

Key words: fiber laser welding technology, laser scanner, non-contact heating welding, galvonometer mirror

INTRODUCTION

Welding technologies, essential for human progress, have significantly evolved. From the earliest technique, forge welding, which used fire to heat and bond metals[1], to advanced methods such as gas, electric arc, shielded gas arc, plasma, and laser welding, each approach utilizes heat to melt metals, creating a joint or weld upon cooling. Traditional methods like gas and arc welding come with inherent limitations. The most notable of these is the difficulty in controlling the depth and area of the weld pool, leading to significant heat loss, which directly impacts the quality and aesthetics of the resulting weld[2]. Moreover, these methods can cause damage to small, delicate parts, limiting their application in precision welding[3].

The advent of laser technology, particularly the use of high-energy laser beams (Light Amplification by Stimulated Emission of Radiation), has offered an efficient solution to these challenges[4]. Despite being a relatively new innovation, introduced in the latter half of the 20th century, laser technology has found wide-ranging applications in fields as diverse as manufacturing, medicine, and the military[5]. Laser welding, while more costly than traditional welding methods, has seen increasing adoption due to its inherent advantages. These include the ability for non-contact heating, precise profile control, localized heat application, minimized heat loss, and the resulting regular, aesthetically pleasing weld. Furthermore, laser welding allows for the welding of small parts without caus-

Cite this article : Nguyen T, Nguyen D, Tran Q. **Research and design two-axis profile scanning control system supporting fiber laser welding technology**. *VNUHCM J. Eng. Technol.* 2026; 9(3):3067-3078.

ing damage, a significant advantage over traditional methods[6]. Laser welding techniques continue to be optimized with research into spatter formation, providing insights that lead to more efficient practices[7]. Studies have also focused on laser welding of specific materials, such as plastics[8], and different metals, revealing economic and technological benefits and the challenges associated with controlling structure and defects[9–13]. Advancements in control systems have improved the performance of scanners used in biomedical technologies[14], while multi-sensor systems enable real-time monitoring of the welding process, ensuring consistent quality[15,16]. Simulations and experiments have provided insights into how oscillation parameters influence the weld's temperature, stress, and distortion, furthering process optimization[17]. Beyond traditional applications, femtosecond laser welding techniques have been used for two-layer vertical welding of glasses, improving microstructure and bonding strength[18]. Other advancements include high-bandwidth fast steering mirrors for better precision and tracking in laser welding[19], autonomous parameter design methods for improved control system performance[20], and the exploration of different oscillating patterns and their effects on weld quality[21,22]. The use of multi-scan picosecond laser welding for transparent materials has led to stronger joints[23]. With the growth in laser welding technology, reliable quality measurement systems are critical, prompting the development of an automatic online system for real-time weld inspection[15].

Traditionally, welding guns with single-shaft mechanisms have been employed for creating profiles in laser welding. Although simple and easy to control, this method is limited to generating basic, circular profiles. However, many applications demand more complex and varied profiles to achieve superior weld quality. To overcome this limitation and meet diverse welding requirements, researchers have proposed a more advanced approach – a two-axis profile scanning control system[24,25]. This method requires more complex fabrication and control than the single-axis method, but allows creation of any two-dimensional profile, let users to have a optimal profile with the best suit to the type of material to be welded, thereby improving the quality of the weld.

In this paper, the authors design and analyze a two-axis profile scanning control system specifically tailored for supporting Fiber Laser Welding Technology. The research aims to develop a model incorporating two reflecting control galvanometer mirrors to create precise laser profiles. Additionally, the study focuses on solving the forward and reverse kinematic problems associated with the system and proposes an advanced algorithm to control its movements. The performance of the proposed model will be validated through simulations on MATLAB, with the ultimate goal of providing a foundation for building a practical two-part profile scanning system for laser welding technology.

METHODOLOGY

Profile scanning system design

As shown in Figure 1, laser welding equipments include main components: laser source, fiber optic cable, 2-axis profile scanning controller, lens, nozzle. The laser source is led to the 2-axis profile scanning control system throught an optical cable. After being reflected on mirrors of the control system, laser beam goes throught focusing lens before comming to the nozzle, which has the function of driving the laser beam to the weld.

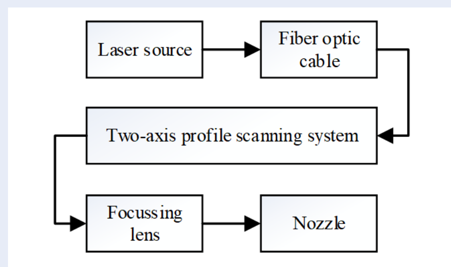

Figure 1: Block diagram of laser welding equipments

In limitation of the research, we only interest the profile scanning system. The model of this control system concist of a laser source S, reflecting galvonometer mirrors G_1 and G_2 and a mounting frame which allows us to unite these items together. By rotating reflecting mirrors in two perpendicular axises, we could create any desired profiles.

For building kinematic equation, we choose a coordinate system OXYZ as shown in the Figure 2. The laser source S is arranged on OY-axis. G_1-mirror spinning around OX-axis is used to expand profile in OY-direction. This mirror reflects beam from the original laser source. G_2-mirror rotates around its axis parallel with OY, reflecting beam from secondary laser source located at point O. By rotation, G2-mirror expand profile in OZ-direction. Two mirrors are arranged that the distance beetween their centers is h, while the distance from this points to profile-screen is d. In a laser welding machine, there is also a lens used

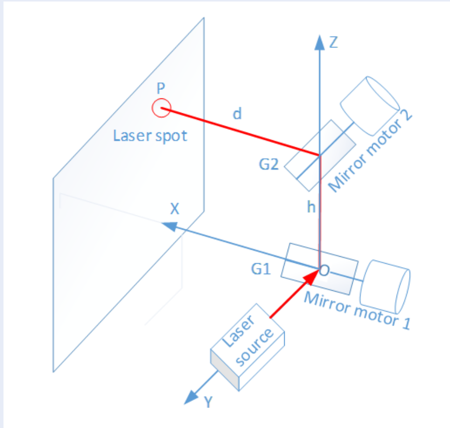

Figure 2: Laser profile scanning model

to focus laser beam, but in inspecting laser profile we could ignore the presence of the lens without affecting its attributes. The model parameters are shown in Table 1.

Rotation angle of G_1-mirror is limitted in a range, which ensuares the ray after G_1-reflection incomming to G_2-plane. When $\alpha = \alpha_1$, the reflected ray coincides with OK_1-ray, while $\alpha = \alpha_2$, it coincides with OK_2-ray. The range of rotation angle of G_1-mirror is defined by (1) and it must not exceed the range of rotation angle of galvanometer.

$$\begin{aligned}\triangle_\alpha &= |\alpha_1 - \alpha_2| = \frac{1}{2} < K_1OK_2 = KOK_1 \\ &= arc\tan\left(KK_1/OK\right) = arc\tan\left(L_{G2}/2h\right)\end{aligned} \quad (01)$$

Where:

$\triangle_\alpha$ - range of rotation angle of G_1-mirror;

O, K, K_1, K_2 - points seen on Figure.3.

Let $L_{G2} =$ 20 mm, $h =$ 30 mm, we have $\triangle_\alpha = 18.5^\circ$.

G_1-mirror is drived to the position, at which reflected ray on G_1 fit to OK-ray. Keep G_1 in this position. When G_2-mirror at position of angle $\beta = \beta_1$, reflected ray on G_2 concides with KP_4-ray. Let rotate G_2-mirror to position $\beta = \beta_2$, reflected ray go fitting to KP_5-ray. The range of rotation angle of G_2-mirror is defined by (2):

$$\begin{aligned}\triangle_\beta &= |\beta_1 - \beta_2| = \frac{1}{2} < P_4OP_5 \\ &= arc\tan\left(PP_4/KP\right) = arc\tan\left(R_z/2d\right)\end{aligned} \quad (02)$$

Where:

$\triangle_\beta$ - range of rotation angle of G_1-mirror;

O, K, P, P_4, P_5 - points seen on Figure 3.

Let $R_Z =$ 30 mm, $d =$ 200 mm, we have $\triangle_\beta = 4.5^\circ$. Let $R_z \to \infty$, $\triangle_\beta \to 90^\circ$. In theory, the range of rotation angle of G_2-mirror can expand to limitation of 90^o, but in practice, it is limitted by the range of rotation angle of galvanometer mirror.

Scanning frequency F_{scan} is limitted in the range of frequency of galvanometer. It must be equal or smaller than F_{max}.

Forward kinematic equation

The used laser source have form of a narrow beam, their cross-section will not change when passing through a mirror system.

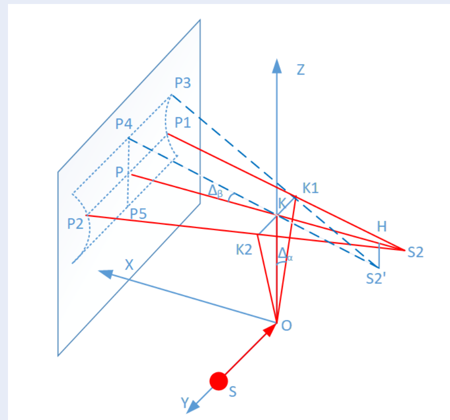

Figure 3: Track of laser throught mirror system

To simplify calculation, we look on laser beam as a single ray projecting to G1-mirror and we inspect profile properties based on this presumption. According to the profile scanning system described in Figure 3, we ensuare that angles of incident of mirrors G_1, G_2 at initial state are $\alpha = 45^o$, $\beta = 45^o$. In this case, the reflected ray from G_1-mirror will coincide with OK-ray, while the reflected ray from G_2-mirror will coincide with KP-ray.

Let G_1-mirror oscillates around the initial position of 45^o and let $\alpha = 45^\circ - \triangle_\alpha/2$, G_2-mirror is fixed at position of angle $\beta = 45^o$, $\triangle_\alpha$is limitted by condition $\triangle_\alpha \leq arc\tan\left(L_{G2}/2h\right)$. From the attributes of mirror reflection, it can be inferred that the reflected OK_1-ray joins OK-ray by an angle of $\triangle_\alpha$. Let S_2 be the image of the secondary laser source (at point O) by G_2-mirror. When $\beta = 45^o$, points S_2, K, P will make a straight line. According to mirror image atributes $KS_2 = KO = h$, and the extension of K_1P_1-ray go through the image S_2. Applying geometric properties, we have:

$$\frac{KK_1}{PP_1} = \frac{S_2K}{S_2P} = \frac{h}{h+d} \quad (03)$$

$$\begin{aligned}&\Rightarrow PP_1 = KK_1\frac{h+d}{h} = h\tan\left(\triangle_\alpha\right)\frac{h+d}{h} \\ &= (h+d)\tan\left(\triangle\alpha\right)\end{aligned} \quad (04)$$

Table 1: Parameters of the model

Parameters	Units	Description
Laser source S:		
Cross section, Scross	mm^2	Cross section of laser beam
Power, Plaser,	W	Power of laser source
G1-mirror:		
Size, WG1 x LG1,	mm	WG1 – edge perpendicular to G1-mirror axis, LG1 - edge parallel with G1-mirror axis.
Angle of incident, α	o	Angle between an incident ray and the normal drawn at the point of contact on G1-mirror.
Rotation angle, $\varphi 1$	o	Angle between an incident ray and G1-mirror plane.
Angular velocity, ω1	o/s	Angular velocity of the G1-mirror around its spinning axis.
G2-mirror:		
Size, LG2 x WG2	mm	WG2 – edge perpendicular to G2-mirror axis, LG2 - edge parallel with G2-mirror axis.
Angle of incident, β	o	Angle between an incident ray and the normal drawn at the point of contact on G2-mirror
Rotation angle, $\varphi 2$	o	Angle between an incident ray and G2-mirror plane
Angular velocity, ω2	o/s	Angular velocity of the G2-mirror around its spinning axis
Mirror arrangements:		
Distance, h	mm	Distance from two centers of mirrors G1 and G2
Distance, d	mm	Distance from mirror centers to profile-screen
Laser profile		
Y- Range, RY	mm	Dimension of profile in Y-direction
Z- Range, RZ	mm	Dimension of profile in Z-direction
Profile area, Sp	mm^2	Area limmited by profile contour
Scanning frequency, Fscan	Hz	Profile scanning frequency
Scanning period, Tscan		Profile scanning period
Galvanometer:		
Limit frequency of galvanometer, Fmax	Hz	Maximum permissible frequency of galvanometer
Working voltage range	V	A range of voltage allowed to apply to galvanometer
Range of rotation angle	o	A range of turnable angles of galvanometer

Let G_1-mirror fix at position α = 45^o, G_2-mirror oscillates around the position of angle 45^o, $\beta = 45^\circ - \triangle_\beta/2$. Image S_2 now oscillates around G_2-spinning axis. Suppose that, image S_2 moves to position $S_2^{'}$ when $\beta = 45^\circ - \triangle_\beta/2$. According to mirror reflection properties, angle $< S_2^{'}KS_2 = PKP_4 = \triangle_\beta$. Reflected KP_4-ray will pass through the image $S_2^{'}$ and $KS_2^{'} = KS_2 = KS_1 = h$. Let H be the projection of $S_2^{'}$on KP-line. Applying geometric properties we have:

$$\frac{S_2^{'}H}{PP_\triangle} = \frac{KH}{KP} = \frac{h\cos\left(\triangle_\beta\right)}{d} \tag{05}$$

$$\begin{aligned} \Rightarrow PP_4 &= S_2^{'}H\frac{d}{h\cos\left(\triangle_\beta\right)} \\ &= h\sin\left(\triangle_\beta\right)\frac{d}{h\cos\left(\triangle_\beta\right)} \\ &= d\tan\left(\triangle_\beta\right) \end{aligned} \tag{06}$$

It is clear that expansion of profile in OZ-direction depends only on distance d and rotation angle of G_2-mirror.

Now, put focus on the case when mirrors G_1 and G_2 oscillate around their initial positions (of angles 45^o):

$$\begin{aligned} \alpha &= 45^\circ - \triangle_\alpha/2 \\ \beta &= 45^\circ - \triangle_\beta/2 \end{aligned} \tag{07}$$

The extension of K_1P_3-ray go throught the image $S_2^{'}$. Apply geometric properties:

$$\frac{KK_1}{P_3P_4} = \frac{S_2^{'}K}{S_2^{'}P_4} = \frac{HK}{HP} = \frac{h\cos\left(\triangle_\beta\right)}{h\cos\left(\triangle_\beta\right)+d} \tag{08}$$

$$\begin{aligned} \Rightarrow P_3P_4 &= KK_1\frac{h\cos\left(\triangle_\beta\right)+d}{h\cos\left(\triangle_\beta\right)} \\ &= h\tan\left(\triangle_\beta\right)\frac{h\cos\left(\triangle_\beta\right)+d}{h\cos\left(\triangle_\beta\right)} \\ &= \left(h+\frac{d}{\cos\left(\triangle_\beta\right)}\right)\tan\left(\triangle_\alpha\right) \end{aligned} \tag{09}$$

Spreading of profile in OY-direction is dependent on d, h and angle $\triangle_\alpha$, $\triangle_\beta$. In conclusion, position of laser spot P_3 on profile-screen is defined by (6) and (9).

Invert kinematic equation

In inverse kinematic equation, we propose a control method to achieve a given profile. As we known any curve can be approximated by parameter function or spline interpolation (cubic spline interpolation, linear spline interpolation, Hermite spline, Bezier spline…). Apply this, a profile $\widehat{P}$ can be devided into n pieces by n points P_1, P_2, …,P_n. Let $\widehat{P_i}$ - a piece of profile between P_i and P_{i+1} (i = 1, 2…, n-1), $\widehat{P_n}$ - piece between P_n and P_1, so we have $\widehat{P} = \left\{\widehat{P_1} \quad \widehat{P_2} \quad \ldots, \widehat{P_n}\right\}$. General funtion describing $\widehat{P_i}$ has form:

$$\widehat{P_i}(t) = \begin{bmatrix} Y_i(t) \\ Z_i(t) \end{bmatrix}, \ t \subset [t_i, \ t_{i+1}] \tag{10}$$

Where t_i – break time of parameter t.

The length of profile contour is determined by fomula:

$$L = \sum_{i=1}^n L_i = \sum_{i=1}^n \int_{t1i}^{t2i} \sqrt{\dot{Y}_i^2(t)+\dot{Z}_i^2(t)}dt \tag{11}$$

In laser welding technology, we expect that speed of laser spot moving along profile remaining unchanged. This speed is then, determinded by fomula:

$$v = L/T_{scan} \tag{12}$$

Let T_i – time span need to be for laser spot moving along $\widehat{P_i}$ pieces.

$$T_i = \frac{L_i}{L}T_{scan} \tag{13}$$

Let t_{real} – real time, $t_{real-1} = T_1$, $t_{real-i} = t_{real-(i-1)}+T_i = T_1+T_2+\ldots+T_i$ – breaks point in real time scale.

Instantaneous speed of laser spot is defined by (14) and according to (12) it is expected to equal L/T_{scan}:

$$\begin{aligned} v &= \frac{dL_i}{dt_{real}} \\ &= \sqrt{\dot{Y}_i^2(t)+\dot{Z}_i^2(t)}\frac{dt}{dt_{real}} = \frac{L}{T_{scan}} \end{aligned} \tag{14}$$

$$\Rightarrow \frac{dt}{dt_{real}} = \frac{L}{T_{scan}\sqrt{\dot{Y}_i^2(t)+\dot{Z}_i^2(t)}} \tag{15}$$

Move coordinate system OXY to profile-screen along vector $\overrightarrow{KP}$. From (4) and (6), we have coordinates of laser spot:

$$Y = \overline{P_4P_3} = \left(h+\frac{d}{\cos\left(\triangle_\beta\right)}\right)\tan\left(\triangle_\alpha\right) \tag{16}$$

$$Z = \overline{PP_4} = d\tan\left(\triangle_\beta\right) \tag{17}$$

Take derivative of two parts of (17) with respect to real time:

$$\begin{aligned} \frac{dZ_i}{dt_{real}} &= \frac{dZ_i}{dt}\frac{dt}{dt_{real}} \\ &= \frac{L\dot{Z}_i}{T_{scan}\sqrt{\dot{Y}_i^2(t)+\dot{Z}_i^2(t)}} = \frac{d\dot{\triangle}_\beta}{\cos^2\left(\triangle_\beta\right)} \end{aligned} \tag{18}$$

$$\Rightarrow \omega_2 = \dot{\triangle}_\beta = \frac{L\dot{Z}_i\cos^2\left(\triangle_\beta\right)}{dT_{scan}\sqrt{\dot{Y}_i^2(t)+\dot{Z}_i^2(t)}} \tag{19}$$

Where: ω_2 - angular velocity of the G_2-mirror.

Similarly, take the derivative of (16) with respect to real time:

$$\frac{dY_i}{dt_{real}} = \frac{dY_i}{dt}\frac{dt}{dt_{real}} = \frac{L\dot{Y}_i}{T_{scan}\sqrt{\dot{Y}_i^2(t)+\dot{Z}_i^2(t)}}$$

$$= \left(h+\frac{d}{\cos(\triangle_\beta)}\right)\frac{d(\tan(\triangle_\alpha))}{dt_{real}} + \tan(\triangle_\alpha)\frac{dt}{dt_{real}}\left(h+\frac{d}{\cos(\triangle_\beta)}\right) \qquad (20)$$

$$\Rightarrow \frac{h\cos(\triangle_\beta)+d}{\cos(\triangle_\beta)}\frac{\triangle_\alpha}{\cos^2(\triangle_\alpha)} + d\tan(\triangle_\alpha)\frac{\sin(\triangle_\beta)}{\cos^2(\triangle_\beta)}\dot{\triangle}_\beta = \frac{L\dot{Y}_i}{T_{scan}\sqrt{\dot{Y}_i^2(t)+\dot{Z}_i^2(t)}} \qquad (21)$$

Or

$$\frac{h\cos(\triangle_\beta)+d}{\cos(\triangle_\beta)}\frac{\omega_1}{\cos^2(\triangle_\alpha)} + d\tan(\triangle_\alpha)\frac{\sin(\triangle_\beta)}{\cos^2(\triangle_\beta)}\omega_2 = \frac{L\dot{Y}_i}{T_{scan}\sqrt{\dot{Y}_i^2(t)+\dot{Z}_i^2(t)}} \qquad (22)$$

Where: $\omega_1 = \dot{\triangle}_\alpha$ - angular velocity of G_1-mirror.

Fomula (22) describes relation between angular velocity of mirrors G_1 and G_2.

Control algorithm

In the model we use two galvanometer mirrors. These equipments have a mirror at one end, and can perform osilation at hight rate. Rotation angle is proportional to voltage applied to galvanometer. Performing algorithm is described by flow chart on Figure 4.

Where N – number of sampling.

In performing we take discreteness of t_{real}, t, Δ_α , Δ_β , ω_1, ω_2. The value of ω_1, $\omega_2$is infered from fumula (19)and (22), while Δ_α , Δ_β are descrete integration of ω_1, ω_2. Digital analog converter converts digital value tovoltage, which is used as input of galvanometer driver. The loop go end when the number of iteration reaches N.

In the algorithm, we can periodly do supplement to rotation angles to remove accumulated difference between calculated rotation angle and the angle defined by the inverse fomula of (16), (17).

$$\triangle_\beta = arc\tan(Z/d) \qquad (18)$$

$$\triangle_\alpha = arc\tan\left(\frac{Y}{h+d/\cos(\triangle_\beta)}\right) \qquad (19)$$

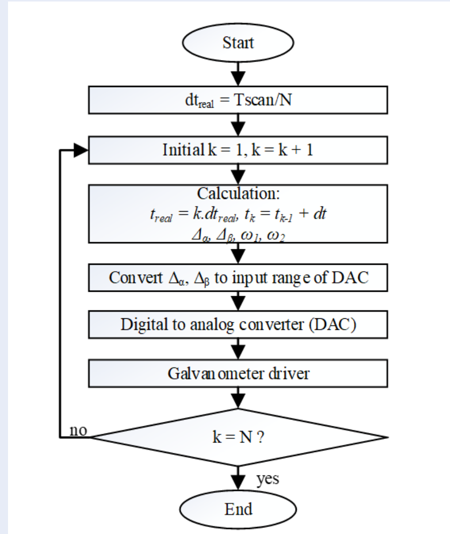

Figure 4: Follow chart of control algorithm

RESULT AND DISCUSSION

For circular profile parameter inputs shown in Table 2. Figure 5 depicts rotation angles over time, while Figure 6 compares obtained circular profile and profile defined by parameter function.

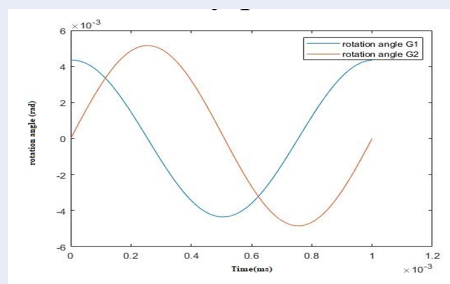

Figure 5: Rotation anglesover real time for circular profile

There is a little bit displacement between these two profile because of descrete integration process of ω_1, ω_2.

Parameters of quadrate profile are described in Table 3.

Figure 7 depicts rotation angles over time, while Figure 8 compares obtained quadrate profile and profile defined by parameter function. They are almost coincident.

For any profile with spline interpolation description, for instance, 8-figured profile with cubic spline interpolation, input parameters are shown in Table 4.

Table 2: Parameters for circular profile

Parameter inputs	Description
T_{scan} = 1ms	Profile scanning period
N = 100	Number of sampling
dt_{real} = 0.01ms	Time sampling
h = 30 mm	Distance from two centers of the mirrors G1 and G2
d = 200 mm	Distance from mirror centers to the profile-screen
$Y = \cos(t)$	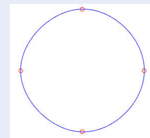
$Z = \sin(t)$	
$t \in [0, 2\pi]$	

Table 3: Parameters for quadrate profile

Parameter inputs	Description
T_{scan} = 1ms	Profile scanning period
N = 100	Number of sampling
dt_{real} = 0.01ms	Time sampling
h = 30 mm	Distance from two centers of mirrors G1 and G2
d = 200 mm	Distance from mirror centers to profile-screen
$\begin{cases} P_1(t) = \begin{cases} Y = t \\ Z = 0 \end{cases}, t \in [0,1] \\ P_2(t) = \begin{cases} Y = 1 \\ Z = t-1 \end{cases}, t \in [1,2] \\ P_3(t) = \begin{cases} Y = 3-t \\ Z = 1 \end{cases}, t \in [2,3] \\ P_4(t) = \begin{cases} Y = 0 \\ Z = t-4 \end{cases}, t \in [3,4] \end{cases}$	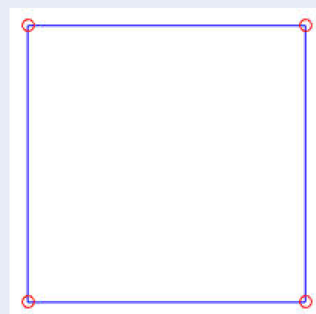

Figure 9 depicts rotation angles over time for 8-figured profile, while Figure 10 compares obtained 8-figured profile and profile defined by parameter function. They are almost coincident. Figure 11 shows obtained profiles with different values of parameter N.

In conclusion, it can be seen that by appling proposed method we retain a good profile that almost close to the desired profile described by parameter function. There is a little bit difference between these two ones because of error in descrete integration. By descresing time sampling (or increasing number of sampling N) we can remove these difference but it leed to increase the volume of calculation.

Tables 5, 6 and 7 sequentially show simulation results for circular profile, quadrate profile and 8-figured profile.

CONCLUSION

In conclusion, this paper has successfully introduced a model of a two-axis profile scanning control system tailored for fiber laser welding technology. The proposed control algorithm has been thoroughly tested through MATLAB simulations, confirming its capability to achieve laser profiles that closely approximate the desired shapes.

The results from the simulations provide strong evidence supporting the feasibility of implementing the proposed control algorithm to construct a practical profile scanning control system for laser welding applications. However, it is essential to consider optimizing the sampling time and ensuring that the control parameters adhere to allowable limits to attain profiles with even higher accuracy.

Table 4: Parameters for quadrate profile

Parameter inputs	Description
T_{scan} = 1ms	Profile scanning period
N = 100	Number of sampling
dt_{real} = 0.01ms	Time sampling
h = 30 mm	Distance from two centers of mirrors G1 and G2
d = 200 mm	Distance from mirror centers to profile-screen
Parameter function (cubic spline interpolation) of 8-figured profile: breaks: [0 1.5708 4.7124 6.2832 7.8540 10.9956 12.5664] pieces: 6, order: 4, dim: 2 coefs: [12×4 double]: -0.1170 -0.0475 1.0000 0 0.1843 -0.6948 0 2.0000 0.1277 -0.5990 -0.0155 1.0000 -0.0369 0.1737 -0.8185 1.0000 -0.1284 0.6050 0.0031 -1.0000 0.1843 -0.1737 -0.8185 -1.0000 -0.1284 0.0000 0.9534 0 -0.1843 0.6948 -0.0000 -2.0000 0.1277 -0.6050 0.0031 1.0000 0.0369 -0.1737 0.8185 -1.0000 -0.1170 0.5990 -0.0155 -1.0000 -0.1843 0.1737 0.8185 1.0000	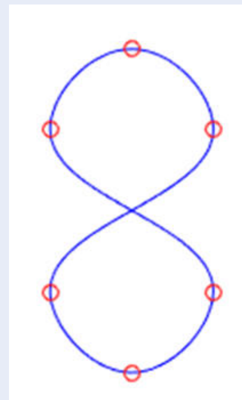

Table 5: The simulation results for circular profile

t_{real} (s)	t(s)	ω_1 (rad/s)	ω_2 (rad/s)	$\triangle_\alpha$ (rad)	$\triangle_\beta$(rad)
0	0	0	31.416	0.0043478	0
1e-05	0.062832	-1.7153	31.354	0.0043478	0.00031416
2e-05	0.12566	-3.4239	31.168	0.0043306	0.0006277
3e-05	0.1885	-5.1189	30.859	0.0042964	0.00093938
……	……	……	……	……	……
0.00098	6.1575	3.4239	31.168	0.0042964	-0.00062522
0.00099	6.2204	1.7153	31.354	0.0043306	-0.00031354
0.001	6.2832	-9.2067e-11	31.416	0.0043478	7.7516e-10

To further enhance the system's performance, future research can focus on refining and fine-tuning the control algorithm, aiming to minimize any disparities between the obtained profiles and the desired shapes. Real-world implementation and validation of the control system within laser welding processes will offer valuable insights and practical validation.

In summary, the research presented in this paper paves the way for the advancement and application of sophisticated profile scanning control systems in fiber laser welding, enabling enhanced welding quality, precision, and adaptability. The ongoing development of such control systems holds the potential to revolutionize laser welding technology and contribute to its broader adoption across various industries.

ABBREVIATIONS

DAC: Analog to digital convertion

CONFLICT OF INTEREST

The authors wish to confirm that there are no know conflicts of interest associated with this publication

Table 6: The simulation results for quadrate profile

t_{real} (s)	t(s)	ω_1 (rad/s)	ω_2 (rad/s)	$\triangle_\alpha$ (rad)	$\triangle_\beta$ (rad)
0	0	17.391	0	0	0
1e-05	0.04	17.391	0	0.00017391	0
2e-05	0.08	17.391	0	0.00034783	0
3e-05	0.12	17.391	0	0.00052174	0
……	……	……	……	……	……
……	……	……	……	……	……
0.00098	3.92	3.602e-11	-20	5.1779e-09	0.0004
0.00099	3.96	1.801e-11	-20	5.1779e-09	0.0002
0.001	4	4.5024e-16	-20	5.1779e-09	4.9999e-09

Table 7: The simulation results for 8-figured profile

t_{real} (s)	t(s)	ω_1 (rad/s)	ω_2 (rad/s)	$\triangle_\alpha$ (rad)	$\triangle_\beta$ (rad)
0	0	52.425	0	0	0.0099997
5e-06	0.060291	52.248	-4.9474	0.00026212	0.0099997
1e-05	0.1208	51.746	-9.669	0.00052337	0.0099749
1.5e-05	0.18132	50.969	-14.108	0.0007821	0.0099266
……	……	……	……	……	……
……	……	……	……	……	……
0.00099	12.446	51.746	9.67	-0.00051922	0.0099228
0.000995	12.506	52.248	4.9482	-0.00026048	0.0099712
0.001	12.567	52.425	-0.017668	7.5671e-07	0.0099959

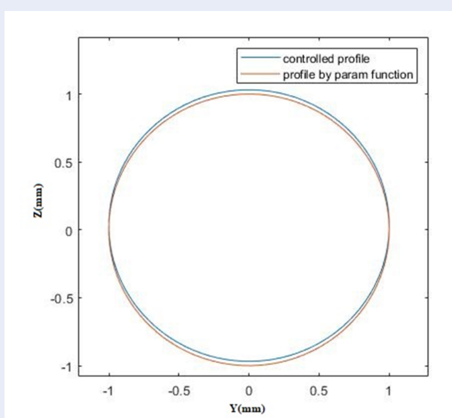

Figure 6: Circular profiles bycontrol and by parameter function

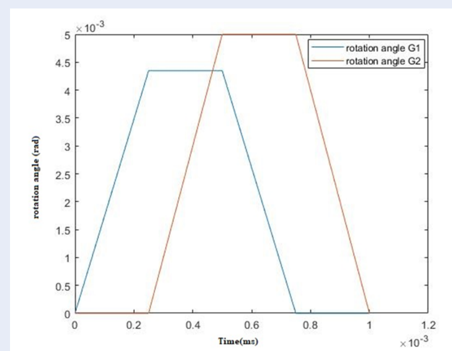

Figure 7: Rotation anglesover real time for quadrate profile

and there has been no significant financial support for this work that could have influenced its outcome.

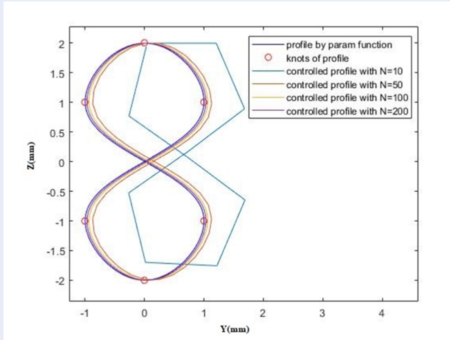

Figure 11: 8-figured profiles with N = 10, 50, 100, 200

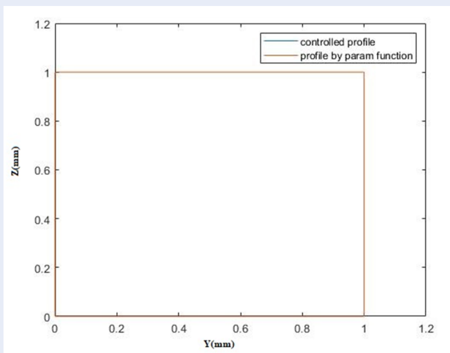

Figure 8: Quadrate profiles bycontrol and by parameter function

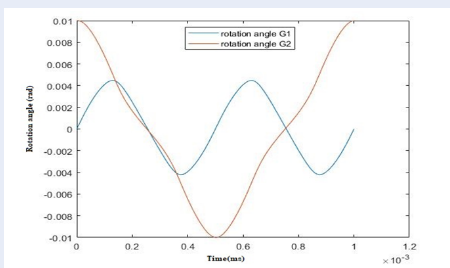

Figure 9: Rotation anglesover real time for 8-figured profile

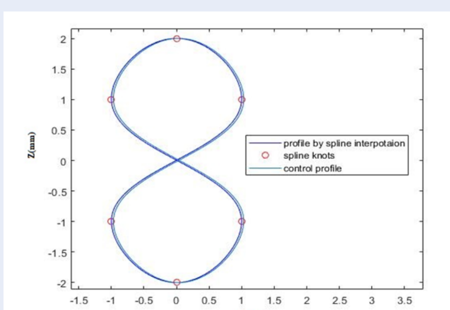

Figure 10: 8-figured profiles bycontrol and by parameter function

AUTHORS' CONTRIBUTION

All authors conceived of the study and participated in its design and coordination and helped to draft the manuscript. The authors read and approved the final manuscript.

Trong-Khuyen Nguyen : wrote the manuscript

Duy-Anh Nguyen : analyzed the results

Quang-Phuoc Tran : designed the study and analyzed the results

ACKNOWLEDGEMENT

We acknowledge the support of time and facilities from Ho Chi Minh City University of Technology(HCMUT), VNU-HCM for this study.

REFERENCES

1. Queneau BR. A History of Metallography. The development of ideas on the structure of metals before 1890. Cyril Stanley Smith. University of Chicago Press, Chicago, Ill., 1960. xxi + 291 pp. $8.50. Science. 1960;132(3440):1656–1657. Available from: https://doi.org/10.1126/science.132.3440.1656.c.
2. Easterling K. Introduction to the Physical Metallurgy of Welding. Butterworth-Heinemann; 1992.
3. DebRoy T, David SA. Physical processes in fusion welding. Reviews of Modern Physics. 1995;67(1):85–112. Available from: https://doi.org/10.1103/RevModPhys.67.85.
4. Steen WM. Laser Material Processing. Springer; 1991. Available from: https://doi.org/10.1007/978-1-4471-3820-4.
5. Ion J. Laser Processing of Engineering Materials: Principles. Procedure and Industrial Application; 2005.
6. Katayama S. Handbook of Laser Welding Technologies. Woodhead Publishing; 2013. Available from: https://doi.org/10.1533/9780857098771.
7. Schweier M, Heins JF, Haubold MW, Zaeh MF. Spatter Formation in Laser Welding with Beam Oscillation. Physics Procedia. 2013;41:20–30. Available from: https://doi.org/10.1016/j.phpro.2013.03.047.
8. Hui L. Research Status and Development Trend of Laser Welding Technology of Plastic; 2013.
9. Kangda H. Weld formation mechanism of fiber laser oscillating welding of austenitic stainless steel; 2015.
10. Lei W, et al.. Effect of beam oscillating pattern on weld characterization of laser welding of AA6061-T6 aluminum alloy; 2016.
11. Xiaobing P. Microstructure and Mechanical Properties of Fiber Laser Welding of Aluminum Alloy with Beam Oscillation; 2019.
12. Fortunato A. Laser Welding of Thin Copper and Aluminum Sheets: Feasibility and Challenges in Continuous-Wave Welding of Dissimilar Metals. Lasers in Manufacturing and Materials Processing; 2019.
13. Kangda H. Laser welding of AZ31B magnesium alloy with beam oscillation; 2019.
14. Corina M, Stefan P, Virgil-Florin D. Classical PID versus predictive control solutions for a galvanometer-based scanner. IEEE; 2015.

15. Deng F, Huang Y, Lu S, Chen Y, Chen J, Feng H, et al. A Multi-Sensor Data Fusion System for Laser Welding Process Monitoring. IEEE Access : Practical Innovations, Open Solutions. 2020;8:147349–57. Available from: https://doi.org/10.1109/ACCESS.2020.3015529.
16. Zhengying J, Zhengang J, Hongchang D. Optical coherence tomography for laser welding applications; 2022.
17. Shenghong Y, et al.. Prediction of temperature field and residual stress of oscillation laser welding of 316LN stainless steel; 2022.
18. Hua T. Two-layer vertical welding of glasses by femtosecond laser through galvo scanner; 2020.
19. Jianpeng Z, Rina N, Tadahiko S. Design and precision tracking control of a high-bandwidth fast steering mirror for laser beam machining. Precision Engineering-journal of The International Societies for Precision Engineering and Nanotechnology; 2021.
20. Eitaro K, Yoshihiro M, Makoto I. Autonomous Parameter Design for Cascade-Structure Feedback Controller Based on Cooperative Optimization Method. IEEJ journal of industry applications. 2021;.
21. Liqun L. Influence of scan paths on flow dynamics and weld formations during oscillating laser welding of 5A06 aluminum alloy; 2020.
22. Cong C. Effects of circular oscillating beam on heat transfer and melt flow of laser melting pool; 2020.
23. Xianshi J, et al.. Multi-scan picosecond laser welding of non-optical contact soda lime glass; 2023.
24. Cheolhee K. Investigation of laser remote welding using disc laser; 2008.
25. Aoyagi I, et al. 2-axis MEMS scanner for a laser range finder. IEEE; 2011. Available from: https://doi.org/10.1109/OMEMS.2011.6031035.

VNUHCM Journal of Engineering and Technology 2026, 9(3):3067-3078

Open Access Full Text Article

Bài nghiên cứu

Nghiên cứu thiết kế hệ thống điều khiển quét biên dạng hai trục hỗ trợ trong công nghệ hàn laser sợi quang

Nguyễn Trọng Khuyên[1], Nguyễn Duy Ánh[2,3], Trần Quang Phước[2,3,*]

Use your smartphone to scan this QR code and download this article

TÓM TẮT

Bài báo trình bày nghiên cứu trên nhiều khía cạnh trong việc thiết kế và phát triển hệ thống điều khiển quét biên dạng hai trục tiên tiến hỗ trợ trong công nghệ hàn laser sợi quang. Hệ thống bao gồm hai gương điện kế đóng vai trò then chốt trong việc điều khiển để đạt được biên dạng laser mong muốn với độ chính xác cao và phức tạp, giải quyết hiệu quả những thách thức cố hữu trong việc kiểm soát ứng dụng nhiệt trong các quy trình hàn trước đây. Bài báo trình bày một cách mạch lạc, đầy đủ mô hình toán học của hệ thống, bao gồm các phương trình động học thuận và nghịch chi phối các góc quay và vận tốc góc của gương. Các phương trình này thiết lập mối quan hệ cơ bản giữa chuyển động của gương và biên dạng laser thu được, giúp hiểu sâu hơn về các cơ chế kiểm soát và điều khiển. Để đảm bảo hiệu suất tối ưu, một thuật toán được nhóm tác giả đề xuất để điều khiển một cách hiệu quả các chuyển động của gương, xem xét cẩn thận thời gian lấy mẫu và các giới hạn vận hành, từ đó cung cấp một cách tiếp cận toàn diện và hiệu quả để kiểm soát hệ thống. Các mô phỏng trên MATLAB được tiến hành để đánh giá hiệu quả và tính chính xác của thuật toán, cung cấp các bằng chứng hữu hình về khả năng đạt được biên dạng laser mong muốn một cách chính xác và có thể điều chỉnh. Phương pháp hàn sử dụng hệ thống điều khiển quét biên dạng hai trục thể hiện những ưu điểm đáng kể so với các phương pháp hàn thông thường, mang lại sự linh hoạt và khả năng kiểm soát tối đa đối với dạng hình học của mối hàn. Tính linh hoạt này cho phép hàn các vật liệu mỏng và các bộ phận phức tạp với độ chính xác vượt trội và tổn thất nhiệt tối thiểu, do đó mở rộng phạm vi ứng dụng trong các ngành công nghiệp khác nhau, bao gồm ô tô, điện tử và thiết bị y tế. Ngoài lĩnh vực hàn, hệ thống điều khiển được phát triển thể hiện tiềm năng to lớn cho các ứng dụng lớn hơn trong xử lý vật liệu, sản xuất phụ gia và các quy trình chế tạo có độ chính xác cao, tiếp tục củng cố vị trí của nó như một công cụ có vai trò biến đổi trong sản xuất và tự động hóa hiện đại. Tóm lại, bài báo nghiên cứu này đóng góp một phần quan trọng cho sự phát triển của công nghệ hàn laser sợi quang bằng cách giới thiệu một hệ thống điều khiển quét biên dạng hai trục tiên tiến. Khả năng tạo ra các biên dạng laser có độ chính xác và tính phức tạp cao của hệ thống này mang đến tiềm năng cách mạng hóa quy trình nối kim loại, trao quyền cho các nhà sản xuất với khả năng linh hoạt và kiểm soát tốt hơn đối với dạng hình học của mối hàn. Đồng thời khả năng ứng dụng rộng rãi của nó trong các ứng dụng có độ chính xác cao mang đến nhiều hứa hẹn cho các ngành công nghiệp, đánh dấu một bước quan trọng đối với việc tiến hành các quy trình sản xuất tiên tiến và hiệu quả.

Từ khoá: Công nghệ hàn laser sợi quang, máy quét laser, công nghệ hàn không tiếp xúc, gương điện kế

[1]*Viện Tự động hóa kỹ thuật quân sự, Việt Nam*

[2]*Khoa Cơ khí, Trường Đại học Bách Khoa TP.HCM, Việt Nam*

[3]*Đại học Quốc gia Thành phố Hồ Chí Minh, Việt Nam*

Liên hệ

Trần Quang Phước, Khoa Cơ khí, Trường Đại học Bách Khoa TP.HCM, Việt Nam

Đại học Quốc gia Thành phố Hồ Chí Minh, Việt Nam

Email: tqphuoc@hcmut.edu.vn

Lịch sử

- Ngày nhận: 06-08-2023
- Ngày sửa đổi: 10-11-2023
- Ngày chấp nhận: 07-08-2025
- Ngày đăng: 03-08-2026

DOI : https://doi.org/10.32508/vnuhcmj-et.v9i3.1141

Trích dẫn bài báo này: Khuyên N T, Ánh N D, Phước T Q. **Nghiên cứu thiết kế hệ thống điều khiển quét biên dạng hai trục hỗ trợ trong công nghệ hàn laser sợi quang**. *VNUHCM J. Eng. Technol.* 2026; 9(3):3067-3078.